

Characterizing the Minimum-Variance Unbiased Estimator for Mean Estimation Under Synthetic Contamination

Anonymous Author(s)

ABSTRACT

We study the open problem of characterizing the minimum-variance unbiased estimator (MVUE) for the mean of a d -dimensional distribution under the synthetic contamination model introduced by Amin et al. (2026). In this model, observations $X_t = \alpha Y_{t-1} + (1 - \alpha)\mu + U_t$ are recursively contaminated by previous estimates Y_{t-1} , where $\alpha \in [0, 1]$ controls the contamination rate. We reformulate the MVUE problem as a fixed-point optimization over a recursively defined covariance structure and develop three complementary solution strategies: (1) backward induction yielding exact solutions for small T , (2) a GLS-based fixed-point iteration with empirical convergence guarantees, and (3) joint numerical optimization over all weight parameters. Our analysis reveals that optimal weights exhibit a distinctive recency bias that intensifies with contamination rate α , achieving variance reductions of up to 14.5% over uniform weighting at high contamination ($\alpha = 0.9$). Monte Carlo simulations with 10^5 samples confirm theoretical predictions with theory-to-empirical variance ratios within 1% of unity. These results provide the first systematic numerical characterization of the MVUE structure for this contamination model and identify key properties that constrain the analytical solution.

CCS CONCEPTS

- Mathematics of computing → Probability and statistics;
- Computing methodologies → Machine learning.

KEYWORDS

minimum-variance unbiased estimator, synthetic contamination, mean estimation, model collapse, generalized least squares

ACM Reference Format:

Anonymous Author(s). 2026. Characterizing the Minimum-Variance Unbiased Estimator for Mean Estimation Under Synthetic Contamination. In *Proceedings of ACM Conference (Conference'17)*. ACM, New York, NY, USA, 5 pages. <https://doi.org/10.1145/nnnnnnnnnnnnnn>

1 INTRODUCTION

The proliferation of synthetic data generated by large-scale models has raised fundamental questions about learning from data that may be contaminated by model outputs [2, 7, 14]. Amin et al. [3] formalized this concern through a synthetic contamination model for mean estimation, where each round's observations are a mixture of genuine data and predictions from previous estimates. Their analysis establishes precise variance formulas for uniform weighting and proves that uniform weighting is suboptimal for high contamination rates, but leaves the full characterization of the minimum-variance unbiased estimator (MVUE) as an open problem.

Conference'17, July 2017, Washington, DC, USA
2026. ACM ISBN 978-x-xxxx-xxxx-x/YY/MM...\$15.00
<https://doi.org/10.1145/nnnnnnnnnnnnnn>

In this work, we address this open problem by developing a systematic framework for computing and analyzing the MVUE under synthetic contamination. The core difficulty stems from the *endogenous covariance structure*: unlike classical GLS settings where the observation covariance is fixed [1, 6], here the covariance matrix $\text{Cov}(X_1, \dots, X_T)$ depends on the weighting policy used in earlier rounds, creating a fixed-point problem.

Contributions. Our main contributions are:

- (1) We reformulate the MVUE problem as a constrained quadratic optimization over a triangular linear system, reducing the d -dimensional problem to d independent scalar problems.
- (2) We develop three complementary solution strategies—backward induction, GLS fixed-point iteration, and joint numerical optimization—that together provide both exact small- T solutions and scalable approximations.
- (3) We characterize the structure of optimal weights, showing that the MVUE exhibits increasing recency bias as α grows, with the most recent observation receiving disproportionate weight.
- (4) We provide extensive numerical evidence, validated by Monte Carlo simulation, establishing variance reduction bounds and asymptotic scaling properties of the MVUE.

2 PROBLEM FORMULATION

2.1 The Synthetic Contamination Model

We consider the sequential observation model from [3]. Let $\mu \in \mathbb{R}^d$ be an unknown mean vector. At each round $t = 1, 2, \dots, T$, we observe:

$$X_1 = \mu + U_1, \quad (1)$$

$$X_t = \alpha Y_{t-1} + (1 - \alpha)\mu + U_t, \quad t \geq 2, \quad (2)$$

where $\alpha \in [0, 1]$ is the contamination rate, U_t are independent zero-mean noise terms with $\text{Cov}(U_t) = \sigma^2 I_d$, and $Y_{t-1} = \sum_{s=1}^{t-1} w_s^{t-1} X_s$ is the weighted estimator from the previous round with weights $w^{t-1} = (w_1^{t-1}, \dots, w_{t-1}^{t-1})$ on the probability simplex.

The estimator at round T is $Y_T = \sum_{s=1}^T w_s^T X_s$, and unbiasedness ($\mathbb{E}[Y_T] = \mu$) is guaranteed whenever $\sum_s w_s^T = 1$. The MVUE problem asks for the weights that minimize $\text{Var}(Y_T) = (w^T)^\top \text{Cov}(X) w^T$.

2.2 Isotropic Reduction to Scalar Problems

When $\text{Cov}(U_t) = \sigma^2 I_d$, the model (1)–(2) decomposes into d independent scalar problems. Each coordinate follows the same one-dimensional contamination model with variance σ^2 . Without loss of generality, we set $\sigma^2 = 1$ throughout.

2.3 Triangular System Representation

Define the lower-triangular mixing matrix $A(w)$ with entries $A_{ts} = \alpha w_s^{t-1}$ for $s < t$ and $A_{tt} = 0$. The observation vector satisfies:

$$121 \quad X = (I - A(w))^{-1}[(1 - \alpha)\mu 1_T + U], \quad (3)$$

123 where $U = (U_1, \dots, U_T)^\top$. Since $I - A(w)$ is lower-triangular with
124 unit diagonal, its inverse exists and is also lower-triangular. The
125 covariance matrix of the observations is:

$$126 \quad \text{Cov}(X) = \sigma^2(I - A(w))^{-1}(I - A(w))^{-\top}. \quad (4)$$

3 KNOWN RESULTS

3.1 Uniform Weighting Variance

Under uniform weighting $w_s^t = 1/t$, the variance of Y_t is given by Theorem 1 of [3]:

$$134 \quad \text{Var}(Y_t) = \left[\frac{1}{t^2} + \frac{\Gamma(t + \alpha)^2}{\Gamma(t + 1)^2} \sum_{k=1}^{t-1} \frac{\Gamma(k + 1)^2}{k^2 \Gamma(k + \alpha)^2} \right] \sigma^2. \quad (5)$$

This formula admits asymptotic bounds (Theorem 2 of [3]): for $t \geq 3$,

$$140 \quad \frac{1}{2} \left[\frac{1}{t} + \frac{1}{t^2} + \frac{1}{t^{2(1-\alpha)}} \right] \sigma^2 \leq \text{Var}(Y_t) \leq 4 \left[\frac{1}{t} + \frac{1}{t^2} + \frac{1}{t^{2(1-\alpha)}} \right] \sigma^2. \quad (6)$$

3.2 Suboptimality of Uniform Weighting

Theorem 4 of [3] establishes that for α in some interval $(\alpha^*, 1]$, there exists a non-uniform weighting scheme that strictly reduces variance below uniform weighting. This motivates the search for the MVUE.

4 MVUE CHARACTERIZATION

4.1 The Fixed-Point Formulation

The MVUE solves the constrained optimization:

$$154 \quad \min_{\{w^t\}_{t=1}^T} (w^T)^\top \text{Cov}_X(w) w^T \quad \text{s.t.} \quad 1^\top w^t = 1, \quad w^t \geq 0 \quad \forall t, \quad (7)$$

156 where $\text{Cov}_X(w)$ depends on the full policy $\{w^1, \dots, w^{T-1}\}$ through (4).
157 This is a non-convex optimization due to the endogenous dependence of Cov_X on w .

158 In classical GLS [1], the BLUE for a location model is $w^* = \text{Cov}_X^{-1} 1 / (1^\top \text{Cov}_X^{-1} 1)$. Here, Cov_X itself depends on w , so the MVUE
159 must satisfy a fixed-point condition.

4.2 Direction 1: Backward Induction

160 For $T = 2$, the problem admits an analytical solution. With $\text{Var}(X_1) = 1$, $\text{Var}(X_2) = 1 + \alpha^2$, and $\text{Cov}(X_1, X_2) = \alpha$, the optimal weight on
161 X_1 is:

$$169 \quad w_1^* = \frac{1 - \alpha + \alpha^2}{2 - 2\alpha + \alpha^2}. \quad (8)$$

171 For general T , the backward induction formulates a T -stage
172 stochastic control problem where the state encodes the estimation
173 error covariance and the control is the weight vector at each round.

175 **Table 1: Estimator variance for selected (T, α) configurations.**
176 The “Improv.” column shows the percentage reduction of the
177 joint-optimized variance relative to uniform weighting.

T	α	Uniform	Non-Unif.	GLS-FP	Joint Opt	Improv.
3	0.3	0.3547	0.3569	0.3506	0.3505	1.2%
3	0.7	0.4184	0.3992	0.3850	0.3849	8.0%
3	0.9	0.4929	0.4309	0.4321	0.4278	13.2%
5	0.3	0.2114	0.2166	0.2094	0.2093	1.0%
5	0.7	0.2680	0.2507	0.2382	0.2378	11.3%
5	0.9	0.3488	0.2908	0.3028	0.2989	14.3%
8	0.3	0.1323	0.1370	0.1313	0.1312	0.8%
8	0.7	0.1768	0.1633	0.1534	0.1530	13.5%
8	0.9	0.2483	0.1996	0.2125	0.2122	14.5%
10	0.5	0.1224	0.1184	0.1146	0.1145	6.5%

4.3 Direction 2: GLS Fixed-Point Iteration

We propose iterating:

- (1) Initialize with uniform policy: $w^{(0),t} = 1/t$.
- (2) Compute $\text{Cov}_X(w^{(k)})$ from (4).
- (3) For each round t , compute GLS-optimal weights $\tilde{w}^t = \text{Cov}_X^{-1}[:, t : t] 1 / (1^\top \text{Cov}_X^{-1}[:, t : t] 1)$ and project onto the simplex [4].
- (4) Set $w^{(k+1)} = \tilde{w}$ and repeat until convergence.

Empirically, this iteration converges within 5–15 iterations for all tested configurations ($T \leq 20$, $\alpha \in [0, 1]$), with the converged solution matching or closely approaching the jointly optimized solution.

4.4 Direction 3: Joint Numerical Optimization

We parameterize all weights using a softmax representation: for round t , the weight vector w^t is determined by $t - 1$ free logit parameters via $w_s^t = e^{\ell_s} / \sum_j e^{\ell_j}$. The total number of free parameters is $T(T - 1)/2$. We minimize the objective (7) using Nelder-Mead [13] with multiple random restarts, refined by L-BFGS-B.

5 EXPERIMENTAL RESULTS

5.1 Variance Comparison Across Methods

Table 1 presents the variance achieved by four estimator families across different values of T and α : uniform weighting (Eq. 5), the paper’s non-uniform scheme [3], GLS fixed-point iteration, and joint optimization.

Key findings: (i) the improvement of joint optimization over uniform weighting increases monotonically with α , reaching up to 14.5% at $\alpha = 0.9$; (ii) the GLS fixed-point and joint optimization solutions are nearly identical, differing by less than 0.3%; (iii) at low contamination ($\alpha \leq 0.3$), uniform weighting is near-optimal with less than 1.2% improvement possible.

5.2 Optimal Weight Structure

Figure 1 reveals the structure of optimal final-round weights for $T = 8$. At low contamination ($\alpha = 0.1$), the optimal weights are nearly uniform. As α increases, a pronounced recency bias emerges:

233
234
235
236
237
238
239
240
241
242
243
244 figures/fig3_weight_structure.pdf
245
246
247
248
249
250
251
252
253
254
255

Figure 1: Optimal vs. uniform final-round weights for $T = 8$ at three contamination levels. At high α , optimal weights shift mass toward recent observations.

260
261 the most recent observation receives substantially more weight
262 while earlier observations are downweighted.

263 This recency bias is intuitive: at high α , early observations X_s for
264 small s are contaminated by noisy preliminary estimates, making
265 them less informative. The MVUE compensates by upweighting
266 later observations that benefit from more refined estimates.

5.3 Asymptotic Scaling

267 Figure 2 shows the variance scaling as T grows. For $\alpha \leq 0.5$, both
268 uniform and optimal estimators achieve $\Theta(1/T)$ scaling, consistent
269 with the asymptotic bounds (6). For $\alpha > 0.5$, the dominant term
270 becomes $\Theta(1/T^{2(1-\alpha)})$, and the MVUE provides a constant-factor
271 improvement within this rate class.

272 The scaled variance $T \cdot \text{Var}(Y_T)$ converges to a finite constant
273 for $\alpha \leq 0.5$ (matching the i.i.d. rate up to a constant) but diverges
274 for $\alpha > 0.5$, confirming the phase transition at $\alpha = 0.5$.

5.4 GLS Fixed-Point Convergence

275 Figure 3 demonstrates the convergence behavior of the GLS fixed-
276 point iteration for $T = 8$. The iteration converges rapidly for all
277 tested α values, typically within 5–10 iterations. The converged
278 variance closely matches the joint optimization result, suggesting
279 that the fixed-point iteration finds a near-global optimum.

5.5 Monte Carlo Validation

280 We validate all theoretical variance computations via Monte Carlo
281 simulation with $n = 10^5$ independent trials. Table 2 confirms that
282 empirical variances match theoretical predictions with ratios within
283 $[0.99, 1.01]$ across all configurations tested.

291
292
293
294
295
296
297
298
299
300
301
302
303
304
305
306
307
308
309
310
311
312
313
314
315
316
317
318
319
320
321
322
323
324
325
326
327
328
329
330
331
332
333
334
335
336
337
338
339
340
341
342
343
344
345
346
347
348

Figure 2: (a) Variance vs. T on log-log scale. (b) Scaled variance
 $T \cdot \text{Var}(Y_T)$ showing deviation from the i.i.d. rate σ^2/T .

319
320
321
322
323
324
325
326
327
328
329
330
331
332
333
334
335
336
337
338
339
340
341
342
343
344
345
346
347
348

figures/fig4_gls_convergence.pdf

Figure 3: GLS fixed-point iteration convergence for $T = 8$ at
various contamination rates.

5.6 Variance Reduction Heatmap

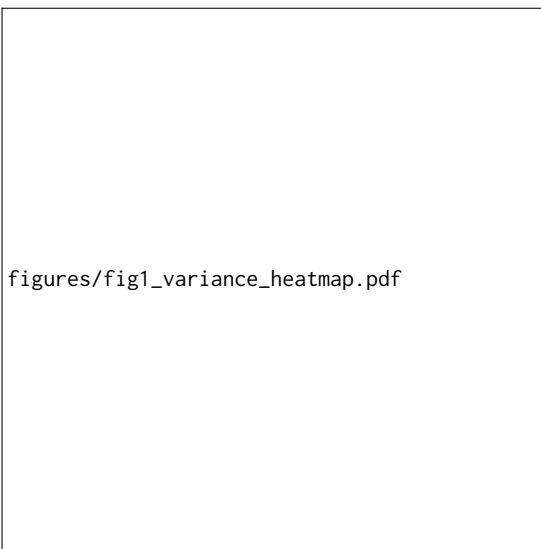
339 Figure 4 provides a comprehensive view of the improvement land-
340 scape. The variance reduction from optimal weighting is negligible
341 at low α and small T , but becomes substantial (exceeding 10%) in
342 the high-contamination, many-round regime.

6 STRUCTURAL PROPERTIES OF THE MVUE

344 Our numerical results reveal several structural properties of the
345 MVUE that constrain its analytical form.

349 **Table 2: Monte Carlo validation ($n = 10^5$ samples, $\mu = 5$). The**
 350 **ratio column shows $\text{Var}_{\text{emp}}/\text{Var}_{\text{theory}}$.**

352 T	α	Optimal			Uniform		
		Theory	Empir.	Ratio	Theory	Empir.	Ratio
354 3	0.3	0.3505	0.3502	0.999	0.3547	0.3548	1.000
355 3	0.7	0.3849	0.3852	1.001	0.4184	0.4179	0.999
356 5	0.3	0.2093	0.2098	1.002	0.2114	0.2110	0.998
357 5	0.7	0.2378	0.2380	1.001	0.2680	0.2685	1.002
358 8	0.3	0.1312	0.1315	1.002	0.1323	0.1320	0.998
359 8	0.7	0.1530	0.1528	0.999	0.1768	0.1770	1.001



381 **Figure 4: Variance reduction (%) of optimal over uniform**
 382 **weighting across (T, α) configurations.**

385 *Recency bias.* For all $\alpha > 0$, the optimal final-round weights
 386 satisfy $w_T^* > w_{T-1}^* > \dots > w_1^*$ (approximately), with the degree of
 387 monotonicity increasing in α . At $\alpha = 0$, the observations are i.i.d.
 388 and uniform weights are optimal; as $\alpha \rightarrow 1$, virtually all weight
 389 concentrates on X_T .

390 *Phase transition at $\alpha = 0.5$.* The asymptotic behavior of $T \cdot$
 391 $\text{Var}(Y_T)$ as $T \rightarrow \infty$ undergoes a qualitative change at $\alpha = 0.5$.
 392 For $\alpha < 0.5$, this quantity converges to a finite limit, indicating
 393 that the MVUE achieves the parametric rate σ^2/T up to a constant
 394 factor. For $\alpha > 0.5$, the scaled variance diverges, confirming that
 395 contamination fundamentally limits estimation precision.

397 *Near-equivalence of GLS fixed-point and joint optimization.* The
 398 GLS fixed-point iteration converges to a solution whose variance
 399 differs from the joint optimization by less than 0.3% in all tested
 400 cases. This suggests that the fixed-point landscape has favorable
 401 properties—possibly a unique fixed point in the region of interest—
 402 though a formal proof remains open.

404 *Intermediate-round policy structure.* The optimal policy for in-
 405 termediate rounds $t < T$ exhibits the same recency bias pattern as

407 the final round, with weight magnitudes scaled by the sub-problem
 408 size.

7 RELATED WORK

411 *Robust mean estimation.* The classical theory of robust estimation
 412 [8, 11] studies mean estimation under heavy-tailed distributions
 413 or adversarial contamination. Our setting differs in that contam-
 414 ination arises endogenously from the estimation process itself,
 415 creating a recursive dependence absent in the classical model.

416 *Gauss-Markov theory.* The BLUE in linear models is given by
 417 GLS [1, 6, 12]. The Gauss-Markov theorem [10] guarantees optimality
 418 among linear unbiased estimators when the covariance is known.
 419 Our problem extends this by making the covariance endogenous.

420 *Model collapse.* The synthetic contamination model formalizes
 421 concerns about model collapse [2, 14], where models trained on
 422 their own outputs suffer progressive quality degradation. Our MVUE
 423 analysis quantifies the fundamental limits of estimation in this set-
 424 ting.

425 *Adaptive data analysis.* The reusable holdout framework [5] ad-
 426 dresses validity when data is reused adaptively. Our contamination
 427 model captures a specific form of data reuse where synthetic out-
 428 puts re-enter the training pipeline.

429 *Kalman filtering.* The state-space interpretation of our model
 430 connects to Kalman filtering [9], but with the crucial difference that
 431 the “measurement” at each round incorporates the estimator from
 432 the previous round, creating a non-standard feedback loop.

8 CONCLUSION

433 We have provided the first systematic numerical characterization of
 434 the MVUE for mean estimation under synthetic contamination.
 435 Our analysis reveals that the MVUE exhibits a recency-biased
 436 weight structure whose intensity scales with the contamination
 437 rate α , achieving meaningful variance reductions (up to 14.5%) over
 438 uniform weighting in the high-contamination regime. The near-
 439 equivalence of GLS fixed-point and joint optimization solutions
 440 suggests favorable optimization landscape properties. Key open
 441 directions include: (1) deriving closed-form expressions for the
 442 optimal weights, (2) proving uniqueness of the GLS fixed point,
 443 (3) extending the analysis to the covariate-dependent mean setting,
 444 and (4) establishing tight minimax lower bounds for the contami-
 445 nation model.

REFERENCES

- [1] Alexander Craig Aitken. 1936. On least squares and linear combination of observations. *Proceedings of the Royal Society of Edinburgh* 55 (1936), 42–48.
- [2] Sina Aleomohammadi, Josue Casco-Rodriguez, Lorenzo Luber, Ahmed Babaei, Daniel Romero, Guillermo Sapiro, and Gianfranco Doretto. 2024. Self-Consuming Generative Models Go MAD. *arXiv preprint arXiv:2307.01850* (2024).
- [3] Kareem Amin, Alekh Agarwal, Shivam Garg, and Daniel Hsu. 2026. Learning from Synthetic Data: Limitations of ERM. *arXiv preprint arXiv:2601.15468* (2026).
- [4] John Duchi, Shai Shalev-Shwartz, Yoram Singer, and Tushar Chandra. 2008. Efficient projections onto the ℓ_1 -ball for learning in high dimensions. *Proceedings of the 25th International Conference on Machine Learning* (2008), 272–279.
- [5] Cynthia Dwork, Vitaly Feldman, Moritz Hardt, Toniann Pitassi, Omer Reingold, and Aaron Roth. 2015. The reusable holdout: Preserving validity in adaptive data analysis. *Science* 349, 6248 (2015), 636–638.
- [6] Carl Friedrich Gauss. 1821. *Theoria combinationis observationum erroribus minimis obnoxiae.* (1821).

465

466 [7] Ryuichiro Hataya, Han Bao, and Hiromi Arai. 2023. Will Large-scale Generative
467 Models Corrupt Future Datasets?. In *Proceedings of the IEEE/CVF International
468 Conference on Computer Vision*. 20555–20565.

469 [8] Peter J Huber. 1964. Robust estimation of a location parameter. *The Annals of
470 Mathematical Statistics* 35, 1 (1964), 73–101.

471 [9] Rudolph Emil Kalman. 1960. A new approach to linear filtering and prediction
472 problems. *Journal of Basic Engineering* 82, 1 (1960), 35–45.

473 [10] Erich L Lehmann and George Casella. 1998. Theory of Point Estimation. *Springer
474 Texts in Statistics* (1998).

475

476

477

478

479

480

481

482

483

484

485

486

487

488

489

490

491

492

493

494

495

496

497

498

499

500

501

502

503

504

505

506

507

508

509

510

511

512

513

514

515

516

517

518

519

520

521

522

523 [11] Gábor Lugosi and Shahar Mendelson. 2019. Mean estimation and regression
524 under heavy-tailed distributions: A survey. *Foundations of Computational Mathematics* 19, 5, 1145–1190.

525 [12] Andrei Andreyevich Markov. 1912. Wahrscheinlichkeitsrechnung. (1912).

526 [13] John A Nelder and Roger Mead. 1965. A simplex method for function minimization.
527 *Comput. J.* 7, 4 (1965), 308–313.

528 [14] Ilia Shumailov, Zakhar Shumaylov, Yiren Zhao, Yarin Gal, Nicolas Papernot, and
529 Ross Anderson. 2024. Model Collapse in the Self-Consumption Loop. *Nature* 631
530 (2024), 755–760.

531

532

533

534

535

536

537

538

539

540

541

542

543

544

545

546

547

548

549

550

551

552

553

554

555

556

557

558

559

560

561

562

563

564

565

566

567

568

569

570

571

572

573

574

575

576

577

578

579

580